Non-linear excitation of quantum emitters in hexagonal boron nitride multiplayers

Cite as: APL Photonics **1**, 091302 (2016); https://doi.org/10.1063/1.4961684
Submitted: 30 June 2016 • Accepted: 15 August 2016 • Published Online: 18 November 2016

Andreas W. Schell, Toan Trong Tran, Hideaki Takashima, et al.

Non-linear excitation of quantum emitters in hexagonal boron nitride multiplayers

Andreas W. Schell,[1,a] Toan Trong Tran,[2] Hideaki Takashima,[1]
Shigeki Takeuchi,[1] and Igor Aharonovich[2]
[1]*Department of Electronic Science and Engineering, Kyoto University, 615-8510 Kyoto, Japan*
[2]*School of Mathematical and Physical Sciences, University of Technology Sydney, Ultimo, New South Wales 2007, Australia*

(Received 30 June 2016; accepted 15 August 2016; published online 1 September 2016)

Two-photon absorption is an important non-linear process employed for high resolution bio-imaging and non-linear optics. In this work, we realize two-photon excitation of a quantum emitter embedded in a two-dimensional (2D) material. We examine defects in hexagonal boron nitride (hBN) and show that the emitters exhibit similar spectral and quantum properties under one-photon and two-photon excitation. Furthermore, our findings are important to deploy two-dimensional hexagonal boron nitride for quantum non-linear photonic applications.
[http://dx.doi.org/10.1063/1.4961684]

Atomic thin, two-dimensional (2D) materials have recently emerged as promising candidates for various nanophotonic and optoelectronic devices, owing to their strong luminescence and unique electronic structure.[1–8] For instance, studies of non-linear absorption or refraction in transition metal dichalcogenides have been promising for applications in mode locking, ultrafast photonics, and optical switching.[9–12]

Hexagonal boron nitride (hBN) is another layered material[13,14] that has recently been subject to an increased research due its ability to host room-temperature quantum emitters.[15–17] While the origin of these emitters is still under investigation, they exhibit remarkable properties such as ultra-high brightness, full polarization, and tunable emission[18] making them very interesting for quantum sensing and optical communications.

In this work, we demonstrate for the first time non-linear excitation of a single emitter in a two-dimensional material, namely, single defects in hBN flakes via two-photon excitation. In two-photon absorption, in contrast to linear one-photon absorption, two photons of twice the one-photon wavelength get absorbed in a non-linear process employing a virtual state.[19,20] This process is highly important in molecular spectroscopy, biological microscopy, and imaging as it reduces the autofluorescence of the surrounding media.[21] Combining two-photon excitation with defects in two-dimensional materials enables atomically thin and lightweight bio-labels, which can be measured with a largely reduced background under excitation and detection in the biological window.[22] Furthermore, since the single quantum emitters are photostable, two photon absorption is a promising pathway to achieve wavelength multiplexing and non-linear quantum photonics with two-dimensional materials.

The setup used to demonstrate two-photon excitation of defects in hBN flakes consists of a home-built laser scanning confocal microscope with a numerical aperture of 0.95 capable of delivering laser pulses of 1 ps duration (measured with an autocorrelator after fibre deliver and filtering) at 780 nm wavelength with a bandwidth of 2 nm or continuous wave light and pulses of about

[a]Electronic mail: schell@kuee.kyoto-u.ac.jp

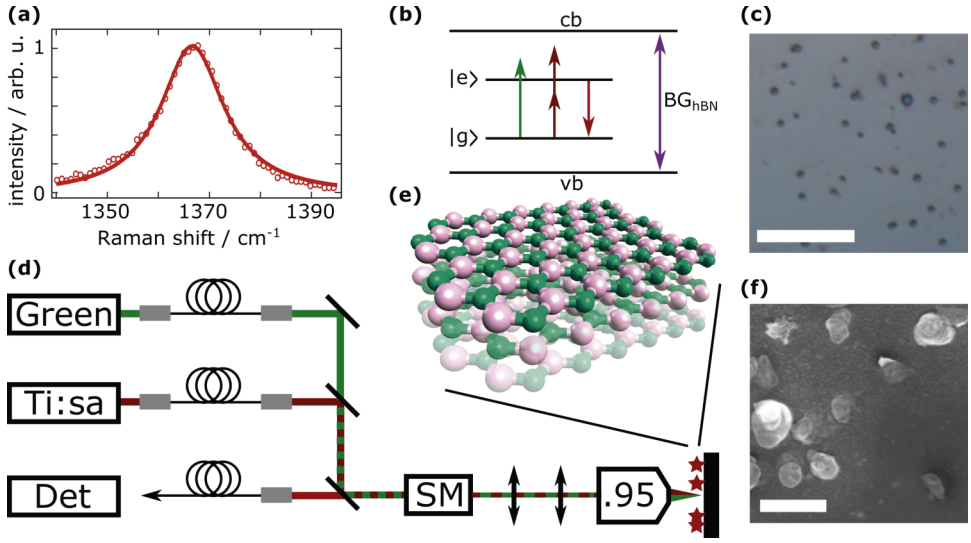

FIG. 1. hBN flakes and optical setup. (a) Raman measurement indicating the presence of multilayer hBN flakes. (b) Simplified level structure of a defect in hBN. In the band gap ($BG_{hBN} = 5.96$ eV) between the conduction and valence bands[23] (cb and vb) lies a two level defect with ground and excited state ($|g\rangle$ and $|e\rangle$). This level can be excited by one or by two photons and will on spontaneous decay emit a photon. (c) Wide field microscope image of the sample. Scalebar is 10 μm. (d) The optical setup used consists of a home-built laser scanning confocal microscope. 532 nm wavelength continuous wave (cw) and pulsed light can be delivered using the upper beam path (Green). Also, light from a titanium sapphire laser (Ti:sa) is delivered to the microscope. The excitation is then coupled to a microscope objective with a numerical aperture of 0.95 and focussed on the sample. Fluorescence light is collected with the same objective lens and coupled to a fibre, which can be plugged to different detectors (Det). A scanning mirror (SM) in a 4f configuration is used for beam scanning. (e) Structure of multilayer hBN (boron rose, nitrogen green). (f) Electron microscope image of the sample. Scalebar is 500 nm.

50 ps at 532 nm wavelength (see Figure 1(c)). Fluorescence light is collected in a spectral window from 561 nm to 700 nm blocking the contributions from scattered laser light at both excitation wavelengths.

The sample investigated was prepared as follows: A native oxide Si (100) substrate was cleaned by ultrasonication in acetone, isopropanol, and ethanol before drop-casting 100 μl of ethanol solution containing pristine h-BN flakes (Graphene Supermarket) of approximately 200 nm in width and 5 nm–50 nm of height onto silicon substrates. This thermal treatment step is employed to increase the optically active defect density.[18] The completely dried sample was then loaded into a fused-quartz tube in a tube furnace (Lindberg Blue™). The tube was evacuated to low vacuum (10^{-3} Torr) by means of a scroll pump then purged for 30 min under 50 sccm of Ar with pressure regulated at 1 Torr. The substrate was then heated at 850 °C for 30 min under 1 Torr of argon. As a last step, the sample was allowed to cool to room-temperature under continuous gas flow. Figure 1(a) shows a Raman spectroscopy measurement performed in order to characterize the sample structure. A single Lorentzian peak fitting yields 1366 cm^{-1} suggesting that the sample is multilayer hBN.[15] The structure of multilayer hBN is shown in Figure 1(d). Defects in this material are expected to have a (simplified) level structure as shown in Figure 1(b). The defects lie in the materials band gap of BG_{hBN} = 5.96 eV[23] and can be excited in the excited state $|e\rangle$ using one or two photons before they decay to the ground state $|g\rangle$ under emission of a photon. The defect was suggested to be an antisite nitrogen-vacancy by a previous study using density functional theory.[15]

Figures 2(a) and 2(b) show confocal micrographs depicting the same region on a sample of hBN flakes excited with pulsed light at 780 nm and continuous wave (cw) excitation at 532 nm wavelength, respectively. Note the different relative fluorescence intensity that the same defects have in both scans. Interestingly, some of the defects are only visible with 532 nm wavelength excitation and invisible under 780 nm excitation wavelength and vice versa. To be able to compare the one-photon with the two-photon excitation, a defect which is clearly visible in both scans (indicated by a white arrow labelled 1) is investigated in the following.

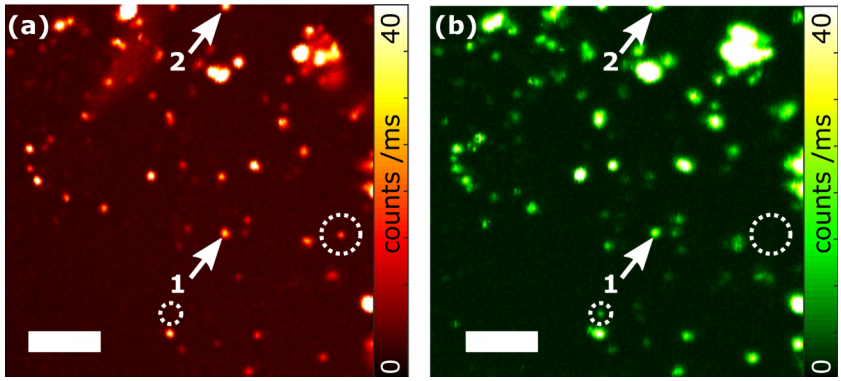

FIG. 2. Two-photon microscopy of hBN flakes. (a) Scan of a sample of hBN flakes using two-photon excitation at a wavelength of 780 nm. (b) Scan of the same area as in (a) using continuous wave excitation at 532 nm wavelength. Numbered arrows indicate defects investigated in the following. Circles indicate two examples of emitter only present in one of the scans. Scale bars are 5 μm.

Figure 3(a) shows the spectrum of this emitter using pulsed 780 nm wavelength excitation. Light in the greyed out wavelength ranges is blocked by optical filters. A clear peak is visible at 670 nm (full width at half-maximum approx. 5 nm). The inset shows the spectrum filtered by a 10 nm bandpass filter centred at the peak wavelength. In Figure 3(b), the same emitter is shown but using 532 nm wavelength cw excitation. Again, a clear peak is visible. The spectrum around the peak differs slightly between (a) and (b), which is attributed to excitations in the surrounding material, which are different when using different excitation wavelengths. The emission corresponds to

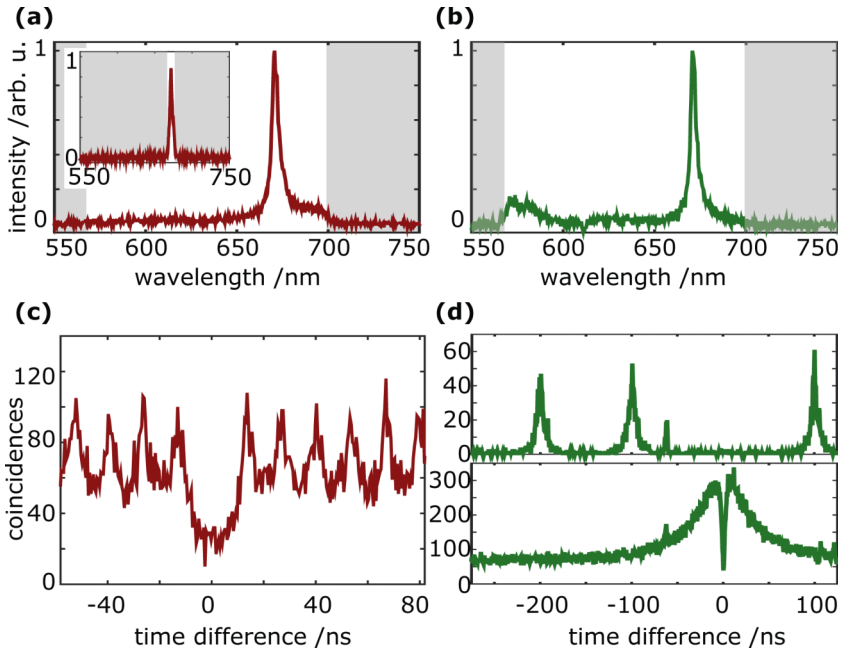

FIG. 3. Spectra and autocorrelation. (a) and (b) Spectrum of the defect labelled 1 in Figures 2(c) and 2(d) using two-photon excitation at 780 nm and one photon excitation at 532 nm wavelength, respectively. The inset in (a) shows the spectrum after a 10 nm bandpass filter centred at the defects emission wavelength had been employed. Both spectra are normalized the same way. Excitation powers were 11.8 mW and 17 μW in (a) and (b), respectively. (c) Intensity autocorrelation measurement using pulsed red excitation. The absence of the peak at zero time delay clearly indicated the presence of a single photon emitter. (d) Intensity autocorrelation measurement using green excitation. The upper part is measured using a pulsed 532 nm wavelength laser while the lower part is measured using a cw laser of the same wavelength. The small peak at −60 ns is an artefact due to cross talk of the avalanche photo-diodes.

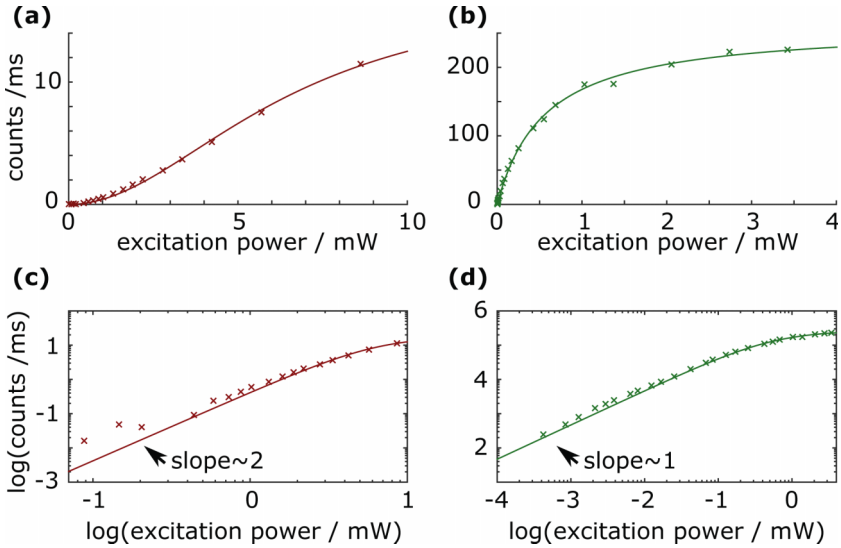

FIG. 4. Excitation power dependence of emission. (a) Dependence of the single photon emission on excitation power using 780 nm wavelength pulsed light. The line is a fit to Equation (2). (b) Same as (a) but using 532 nm wavelength cw excitation light. The line is a fit to Equation (1). (c) and (d) double logarithmic plots of the data in (a) and (b), respectively. Note the different slopes of the logarithm of Equations (1) and (2) for low excitations powers. Integration for each data point was 10 s.

an isolated defect embedded in a hBN lattice, in accordance to previous results.[15,18] Figures 3(c) and 3(d) show intensity autocorrelation measurements of the photons from the defect with pulsed red and cw and pulsed green excitation, respectively. In these measurements, the 10 nm bandpass filter was employed in order to suppress background photons. Excitation power was 13.2 mW in (c), which corresponds to approximately twice the saturation power I_s (see Figure 4 and Equation (2)). All excitation powers are measured before the beam enters the microscope objective. The measurements confirm that the addressed defect is a true single photon emitter. The complete absence of a peak in the coincidences at zero time delay for pulsed green excitation in the upper part of (d) indicates the purity of the emitter. From this measurement, also the excited state lifetime of the emitter is extracted to be 10.4 ns. The cw green excitation measurement is taken in the saturated regime at an excitation power of 3.7 mW. Besides the antibunching dip (with a depth limited by our detectors' timing resolution), it shows a pronounced bunching behaviour. Such a behaviour appears if there are higher correlations between photons emitted with a medium time difference (compared to the excited state lifetime) than with a large time difference. This indicates the presence of an additional state or configuration which does not emit photons at the detection wavelength. Causes for this are, for example, by intersystem crossing[24,25] or spectral diffusion.[26,27]

Using pulsed red excitation, also in the saturated regime (see Figure 3(c)) this behaviour is not visible, an indication that due to different excitation wavelengths different levels in the defect are addressed that are not included in the simplified level scheme in Figure 1(b). One possible explanation to this is that the shelving state present gets depopulated by the red laser in a kind of re-pumping process.[25]

In order to get a better understanding of the defect and to prove that indeed two-photon excitation is the dominant excitation process using 780 nm wavelength pulsed light, the dependence of the number of photons emitted on the excitation power was measured. For a one-photon process, (denoted by subscript 1) this dependence follows[28]

$$R = R_{\mathrm{inf},1}\frac{\left(\frac{I}{I_{s,1}}\right)}{\left(\frac{I}{I_{s,1}}\right)+1}, \tag{1}$$

where R is the photon emission rate, I is the excitation intensity, $I_{s,1}$ is the saturation intensity, and $R_{\mathrm{inf},1}$ is the maximum photon emission rate. For a two-photon process (denoted by subscript 2),

where the dependence on intensity is quadratic, the number of emitted photons follows

$$R = R_{\mathrm{inf},2} \frac{\left(\frac{I}{I_{s,2}}\right)^2}{\left(\frac{I}{I_{s,2}}\right)^2 + 1}. \tag{2}$$

The corresponding measurements are shown in Figure 4. In Figures 4(a) and 4(c), the measurements using 780 nm wavelength pulsed light are shown on a linear and double logarithmic scale, respectively. A fit to Equation (2) (drawn through line) yields $R_{\mathrm{inf},2} = 18\,000/\mathrm{s}$ and $I_{s,2} = 6.5$ mW. In Figures 4(b) and 4(d), the measurements using 532 nm wavelength cw light are shown on a linear and double logarithmic scale, respectively. A fit to Equation (1) (drawn through line) yields $R_{\mathrm{inf},1} = 260\,000/\mathrm{s}$ and $I_{s,1} = 0.56$ mW. All fits were performed using a least squares algorithm.

While these measurements prove the two-photon excitation using the red laser, there is a large difference in the maximum count rate R_{inf} between the different modes of excitation. This difference of over one magnitude cannot be explained by different setup configuration or due to chromatic aberrations since the emitted photons have the same wavelength in both cases. Bad alignment of the excitation hence would only influence I_s. Therefore, as in the antibunching measurements, we assume that there are additional states present, which get populated differently depending on the excitation mode. Interestingly, the emitter is brighter under green excitation, which is the opposite one would expect if it gets de-shelved by the red laser. This is an indication that the defects in hBN possess a complicated level structure. Further evaluation of the level structure lies beyond the scope of this paper, but we want to point out that this makes defects in hBN highly interesting for applications in quantum optics, where it is highly desired to have the possibility to address different levels.

Figure 5(a) shows the spectrum of the defect labelled 2 in Figure 2 under pulsed red excitation. On a broad background, there are many lines visible. As expected from this, in the second order autocorrelation function shown in Figure 5(b), the peak at zero is still present, yet reduced, which means that more than one emitter contributes to the signal measured. This shows that even on a small scan as the scan in Figure 2, many quantum emitters can be seen. While many single emitters are observed using single photon (green) excitation that is not necessarily the case for two-photon excitation. Due to the high excitation powers used for two-photon measurements, stability of the defects becomes an issue. While some emitters, as emitter 1, were long term stable, many others got destroyed by the laser. One way to solve this in future experiments would be to use a laser pulse shorter than the one of 1 ps used here, which will reduce thermal load on the emitters considerably. Nevertheless, as shown in Figure 5, it is possible to find more emitters that behave non-classically.

In conclusion, we have demonstrated two-photon excitation of single quantum emitters in two-dimensional hexagonal boron nitride. To our knowledge, this is the first time that such a measurement has successfully performed on a two-dimensional material or a single defect in general. While in our experiment, we used flakes with a lateral dimension of 200 nm, the small size of the

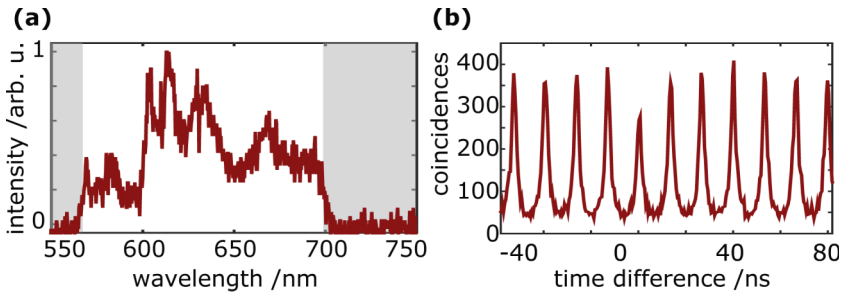

FIG. 5. Spectrum and second order autocorrelation of defect 2. (a) Spectrum of the defect labelled 2 in Figure 2 under pulsed red excitation. Many lines are visible on a broad background. (b) Corresponding second order autocorrelation measurement. The peak at zero time delay is considerably reduced proofing the non-classicality of the light emitted. This clearly shows that even in a small scan area as in Figure 2 many quantum emitters capable of two-photon excitation can be found.

proposed defect structures of just a few atoms[15] suggests that much smaller flake sizes are possible. Such small sizes can be achieved, for example, by ball milling.[29] This demonstrates the capabilities of two-dimensional materials for potential use as small and stable bio-markers operating in the biological window wavelength range. Our findings achieved under different excitation conditions give first insights in the defects' level structure, which is a prerequisite for understanding the defects properties such as quantum efficiency and absorption cross section and an important milestone on the way to non-linear quantum photonics.

The work was supported in part by the Australian Research Council (ARC) Discovery Early Career Research Award (No. DE130100592) and the ARC Research Hub for Integrated Device for End-user Analysis at Low-levels (Grant No. IH150100028), FEI Company and by the AOARD Grant No. FA2386-15-1-4044, MEXT/JSPS KAKENHI Grant Nos. 26220712 and 21102007, Special Coordination Funds for Promoting Science and Technology, and the Cooperative Research Program of "Network Joint Research Center for Materials and Devices." A.W.S. is funded by the Japanese Society for the Promotion of Science through a fellowship for overseas researchers.

[1] F. Xia, H. Wang, D. Xiao, M. Dubey, and A. Ramasubramaniam, "Two-dimensional material nanophotonics," Nat. Photonics **8**, 899–907 (2014).
[2] J. Yang, R. Xu, J. Pei, Y. W. Myint, F. Wang, Z. Wang, S. Zhang, Z. Yu, and Y. Lu, "Optical tuning of exciton and trion emissions in monolayer phosphorene," Light: Sci. Appl. **4**, e312 (2015).
[3] H. R. Gutiérrez, N. Perea-López, A. L. Elías, A. Berkdemir, B. Wang, R. Lv, F. López-Urías, V. H. Crespi, H. Terrones, and M. Terrones, "Extraordinary room-temperature photoluminescence in triangular WS_2 monolayers," Nano Lett. **13**, 3447–3454 (2012).
[4] Y. Gong, J. Lin, X. Wang, G. Shi, S. Lei, Z. Lin, X. Zou, G. Ye, R. Vajtai, B. I. Yakobson *et al.*, "Vertical and in-plane heterostructures from WS_2/MoS_2 monolayers," Nat. Mater. **13**, 1135–1142 (2014).
[5] A. Splendiani, L. Sun, Y. Zhang, T. Li, J. Kim, C.-Y. Chim, G. Galli, and F. Wang, "Emerging photoluminescence in monolayer MoS_2," Nano Lett. **10**, 1271–1275 (2010).
[6] X. Liu, T. Galfsky, Z. Sun, F. Xia, E.-c. Lin, Y.-H. Lee, S. Kéna-Cohen, and V. M. Menon, "Strong light–matter coupling in two-dimensional atomic crystals," Nat. Photonics **9**, 30–34 (2015).
[7] G. Fiori, F. Bonaccorso, G. Iannaccone, T. Palacios, D. Neumaier, A. Seabaugh, S. K. Banerjee, and L. Colombo, "Electronics based on two-dimensional materials," Nat. Nanotechnol. **9**, 768–779 (2014).
[8] P. Tonndorf, R. Schmidt, R. Schneider, J. Kern, M. Buscema, G. A. Steele, A. Castellanos-Gomez, H. S. van der Zant, S. M. de Vasconcellos, and R. Bratschitsch, "Single-photon emission from localized excitons in an atomically thin semiconductor," Optica **2**, 347–352 (2015).
[9] D. Li, W. Xiong, L. Jiang, Z. Xiao, H. Rabiee Golgir, M. Wang, X. Huang, Y. Zhou, Z. Lin, J. Song *et al.*, "Multimodal nonlinear optical imaging of MoS_2 and MoS_2-based van der Waals heterostructures," ACS Nano **10**, 3766–3775 (2016).
[10] Y. Li, N. Dong, S. Zhang, X. Zhang, Y. Feng, K. Wang, L. Zhang, and J. Wang, "Giant two-photon absorption in monolayer MoS_2," Laser Photonics Rev. **9**, 427–434 (2015).
[11] S. Zhang, N. Dong, N. McEvoy, M. OBrien, S. Winters, N. C. Berner, C. Yim, Y. Li, X. Zhang, Z. Chen *et al.*, "Direct observation of degenerate two-photon absorption and its saturation in WS_2 and MoS_2 monolayer and few-layer films," ACS Nano **9**, 7142–7150 (2015).
[12] D.-S. Tsai, K.-K. Liu, D.-H. Lien, M.-L. Tsai, C.-F. Kang, C.-A. Lin, L.-J. Li, and J.-H. He, "Few-layer MoS_2 with high broadband photogain and fast optical switching for use in harsh environments," ACS Nano **7**, 3905–3911 (2013).
[13] J. D. Caldwell, A. V. Kretinin, Y. Chen, V. Giannini, M. M. Fogler, Y. Francescato, C. T. Ellis, J. G. Tischler, C. R. Woods, A. J. Giles *et al.*, "Sub-diffractional volume-confined polaritons in the natural hyperbolic material hexagonal boron nitride," Nat. Commun. **5**, 5221 (2014).
[14] L. Song, L. Ci, H. Lu, P. B. Sorokin, C. Jin, J. Ni, A. G. Kvashnin, D. G. Kvashnin, J. Lou, B. I. Yakobson *et al.*, "Large scale growth and characterization of atomic hexagonal boron nitride layers," Nano Lett. **10**, 3209–3215 (2010).
[15] T. T. Tran, K. Bray, M. J. Ford, M. Toth, and I. Aharonovich, "Quantum emission from hexagonal boron nitride monolayers," Nat. Nanotechnol. **11**, 37–41 (2016).
[16] N. R. Jungwirth, B. Calderon, Y. Ji, M. G. Spencer, M. E. Flatté, and G. D. Fuchs, "Temperature dependence of wavelength selectable zero-phonon emission from single defects in hexagonal boron nitride," preprint arXiv:1605.04445 (2016).
[17] R. Bourrellier, S. Meuret, A. Tararan, O. Stephan, M. Kociak, L. H. G. Tizei, and A. Zobelli, "Bright UV single photon emission at point defects in *h*-BN," Nano Lett. **16**, 4317 (2016).
[18] T. T. Tran, C. ElBadawi, D. Totonjian, C. J. Lobo, G. Grosso, H. Moon, D. R. Englund, M. J. Ford, I. Aharonovich, and M. Toth, "Robust multicolor single photon emission from point defects in hexagonal boron nitride," ACS Nano, Article ASAP (2016).
[19] W. Kaiser and C. G. B. Garrett, "Two-photon excitation in CaF_2: Eu^{2+}," Phys. Rev. Lett. **7**, 229–231 (1961).
[20] D. M. Friedrich, "Two-photon molecular spectroscopy," J. Chem. Educ. **59**, 472 (1982).
[21] W. Denk, J. H. Strickler, and W. W. Webb, "Two-photon laser scanning fluorescence microscopy," Science **248**, 73–76 (1990).
[22] R. Weissleder, "A clearer vision for *in vivo* imaging," Nat. Biotechnol. **19**, 316–317 (2001).
[23] G. Cassabois, P. Valvin, and B. Gil, "Hexagonal boron nitride is an indirect bandgap semiconductor," Nat. Photonics **10**, 262 (2016).

[24] J. Bernard, L. Fleury, H. Talon, and M. Orrit, "Photon bunching in the fluorescence from single molecules: A probe for intersystem crossing," J. Chem. Phys. **98**, 850–859 (1993).
[25] C. Kurtsiefer, S. Mayer, P. Zarda, and H. Weinfurter, "Stable solid-state source of single photons," Phys. Rev. Lett. **85**, 290–293 (2000).
[26] G. Sallen, A. Tribu, T. Aichele, R. André, L. Besombes, C. Bougerol, M. Richard, S. Tatarenko, K. Kheng, and J.-P. Poizat, "Subnanosecond spectral diffusion measurement using photon correlation," Nat. Photonics **4**, 696–699 (2010).
[27] J. Wolters, N. Sadzak, A. W. Schell, T. Schröder, and O. Benson, "Measurement of the ultrafast spectral diffusion of the optical transition of nitrogen vacancy centers in nano-size diamond using correlation interferometry," Phys. Rev. Lett. **110**, 027401 (2013).
[28] L. Novotny and B. Hecht, *Principles of Nano-Optics* (Cambridge University Press, 2012).
[29] Y. Lin and J. W. Connell, "Advances in 2D boron nitride nanostructures: Nanosheets, nanoribbons, nanomeshes, and hybrids with graphene," Nanoscale **4**, 6908–6939 (2012).